

Numerical Robustness of Single Layer method with Fourier basis in 2D multiple obstacle scattering.

Hélène Barucq¹ Ha Pham¹ Juliette Chabassier¹ Sébastien
Tordeux¹

Wave 2017 Conference, University of Minnesota,
May 2017.

¹Inria SudOuest Research Center - Magique 3D team project, Pau, France.

Overview

- 1 Introduction of method
- 2 Comparison with Finite Element Method
- 3 Solver's robustness comparison
 - Closely spaced obstacles
 - Far away obstacles
- 4 Application to inversion : initial results
 - No noise
 - 23dB Noise

Plan

1 Introduction of method

Multiple obstacle scattering as Exterior Boundary Value problems

Propagation of acoustic waves of freq. f in a hom. medium with sound speed c .

$$u_{\text{total}} = u_{\text{inc}} + u_{\text{scatt}}.$$

1. PDE satisfied by u_{scatt} outside of the obstacles:

$$(-\Delta - \kappa^2) u_{\text{scatt}} = 0, \quad \kappa = \frac{2\pi f}{c}.$$

For transmission prob, $(-\Delta - \kappa_{\text{int}})u_{\text{int}} = 0$ inside obstacles.

2. Conditions on the boundary of the obstacles:

$$\text{Dirichlet} \quad u_{\text{total}} = 0$$

$$\text{Neumann} \quad \partial_n u_{\text{total}} = 0$$

$$\text{Impedance} \quad \partial_n u_{\text{total}} + i\lambda u_{\text{total}} = 0$$

$$\text{Transmission} \quad u_{\text{total}} - u_{\text{int}} = 0; \quad \partial_n u_{\text{total}} - \mu u_{\text{int}} = 0$$

3. (Outgoing) Sommerfeld radiation condition at ∞ :

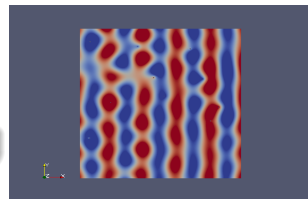
$$\lim_{r \rightarrow \infty} \sqrt{r} (\partial_r u_{\text{scatt}} - i\kappa u_{\text{scatt}}) = 0 \quad ; \quad r = |x|$$

Time-harmonic Planewave :

$$u_{\text{pw}}(x) \exp(-i 2\pi f t)$$

$$u_{\text{pw}}(x) = \exp(\kappa x \cdot \begin{pmatrix} \cos \alpha_{\text{inc}} \\ \sin \alpha_{\text{inc}} \end{pmatrix})$$

$$\alpha_{\text{inc}} = 0^\circ, \quad 2\pi f = 1.0, \quad \kappa = 1.0.$$



$\exists!$ solution for the exterior BVPs (all parameters > 0).

Single layer potential formulation.

Ext. Dir. Prob : $u_{\text{total}} = u_{\text{inc}} + u_{\text{scatt}}$;
 $(-\Delta - \kappa^2)u_{\text{scatt}} = 0$ outside of Obs;
 u_{scatt} satisfies Som. rad. cond;
 $u_{\text{scatt}}|_{\Gamma_{\text{Obs}}} = -u_{\text{inc}}.$

Integral Equation (IE)

$$u_{\text{scatt}} = \sum_{J=1}^{N_{\text{Obs}}} u_{\text{scatt},J};$$

$$u_{\text{scatt},J} := \tilde{S}_J v_J = \int_{\Gamma_J} G_{\kappa}(x,y) v_J(y) ds(y).$$

IE Problem: Find densities v_J so that

$$\sum_{J=1}^{N_{\text{Obs}}} S_{IJ} v_J = -\gamma_{0,I} u_{\text{inc}}, \quad I = 1, \dots, N_{\text{Obs}};$$

$$S_{IJ} = \gamma_{0,I} \tilde{S}_J; \quad \gamma_{0,I} \text{ 0-th trace along } \Gamma_I.$$

Variational IE : Find v_J so that

$$\sum_{J=1}^{N_{\text{Obs}}} (S_{IJ} v_J, \phi) = \langle -u_{i,I}, \phi \rangle_{H^{1/2}(\Gamma_I), H^{-1/2}(\Gamma_I)}$$

$$\forall I = 1, \dots, N_{\text{Obs}} \text{ and test func } \phi \in H^{-1/2}(\Gamma_I).$$

Variational
formulation

Boundary Element
(BEM)

Variational IE for test func in
finite-dim subspaces $\{V_{I,m}\}$
approximating $H^{-1/2}(\Gamma_I)$

Fourier Series
Single Layer

Curved BEM
Galerkin

$$V_m \text{ is given by } \left\{ \sum_{k=-m}^m a_k e^{ik\theta} \right\}$$

V_m given by piecewise
 P_m functions

Disc-shaped obstacles

Multipole

0th order approximation

0th order approximation

Foldy isotropic
point scattering

Fourier Series Single Layer method.

The scattered and approx. wave

$$u_{\text{scatt}} = \sum_{J=1}^{N_{\text{Obs}}} u_{\text{scatt};J},$$

$$u_{\text{scatt},h} = \sum_{J=1}^{N_{\text{Obs}}} u_{h,\text{scatt};J}.$$

The exact and app. wave scattered by Obs J

$$u_{\text{scatt};J} = \tilde{S}_J v_J; \quad u_{h,\text{scatt};J} = \tilde{S}_J v_{h,J}.$$

In basis elements

$$\mathbf{w}_{J,k}(x) = e^{ik\theta_J(x)},$$

$$u_{\text{scatt};J} = \sum_{k \in \mathbb{Z}} v_{J,k} \tilde{S}_J \mathbf{w}_{J,k}$$

$$u_{h,\text{scatt};J} = \sum_{k=-m}^m v_{J,k} \tilde{S}_J \mathbf{w}_{J,k}.$$

The unknowns are the Fourier coeff. of density v_J

$$V = (V_{J,k}), \quad k \in \mathbb{Z}, 1 \leq J \leq N_{\text{Obs}},$$

and the truncated ones for the approx. $v_{h,J}$.

$$V_h = (V_{J,k}), \quad -m \leq k \leq m, \quad 1 \leq J \leq N_{\text{Obs}}.$$

For $\alpha = D, N, \text{Im}, T$, they solve

$$\mathbf{A}_\alpha V = F_\alpha, \quad \mathbf{A}_{h,\alpha} V_h = F_{\alpha,h}.$$

$$\mathbf{A}_\alpha = \begin{pmatrix} \mathbf{A}_{11} & \mathbf{A}_{12} & \cdots & \mathbf{A}_{1(N-1)} & \mathbf{A}_{1N} \\ \mathbf{A}_{21} & \mathbf{A}_{22} & \cdots & \mathbf{A}_{2(N-1)} & \mathbf{A}_{2N} \\ \vdots & \vdots & \ddots & \vdots & \vdots \\ \mathbf{A}_{(N-1)1} & \mathbf{A}_{(N-1)2} & \cdots & \mathbf{A}_{(N-1)(N-1)} & \mathbf{A}_{(N-1)N} \\ \mathbf{A}_{N1} & \mathbf{A}_{N2} & \cdots & \mathbf{A}_{N(N-1)} & \mathbf{A}_{NN} \end{pmatrix}$$

$\mathbf{A}_{h,\alpha}$ square matrix of size $(2m+1) \times N_{\text{Obs}}$.

$\mathbf{A}_{\alpha,l}$ self-interaction of obstacle l

$\mathbf{A}_{\alpha,lJ}$ diffraction by obs. l of wave emitted by obs. J

Multi-scattering matrix coefficient for circular obstacles.

For circular obstacles, single-layer densities $\tilde{S}_J \mathbf{w}_{J,k}$ can be written in **multipole expansions**,

$$(\tilde{S}_J \mathbf{w}_{J,k})(x) = \frac{i\pi \mathbf{r}_J}{2} J_k(\kappa \mathbf{r}_J) \underbrace{H_k^{(1)}(\kappa r_J(x)) e^{ik\theta_J(x)}}_{\text{multiple pole of order } k \text{ placed at the center of } \mathcal{O}_J}.$$

N_{Obs} circular obstacles.

Obstacle \mathcal{O}_I centered at \mathbf{x}_I with radius \mathbf{r}_I

For Dirichlet : Same obstacle interaction

$$(\mathbf{A}_{D;I})_{kl} = i\pi \mathbf{r}_I H_k^{(1)}(\kappa \mathbf{r}_I) J_k(\kappa \mathbf{r}_I) \delta_{kl}, \quad k, l \in \mathbb{Z}.$$

Relative polar coordinates

$$(r_J(\cdot), \theta_J(\cdot))$$

with respect to \mathbf{x}_J

$$(\mathbf{A}_{D;IJ})_{kl} = i\pi \mathbf{r}_J e^{i(l-k)\theta_{\mathbf{x}_J}(\mathbf{x}_I)} H_{l-k}^{(1)}(\kappa \mathbf{d}_{IJ}) J_k(\kappa \mathbf{r}_I) J_l(\kappa \mathbf{r}_J),$$

$$\mathbf{d}_{IJ} = |\mathbf{x}_I - \mathbf{x}_J| \quad ; \quad k, l \in \mathbb{Z}.$$

$$x = \mathbf{x}_J + r_J(x)(\cos \theta_J(x), \sin \theta_J(x))$$

Right-hand-side corresponding to planewave

$$\mathbf{x}_I = \mathbf{x}_J + \mathbf{d}_{IJ}(\cos \theta_{JI}, \sin \theta_{JI})$$

$$u_{\text{pw}}(x) = \exp(i \kappa x \cdot (\cos \alpha_{\text{inc}}, \sin \alpha_{\text{inc}})),$$

$$(\mathbf{F}_{D;I})_k = -2 u_{\text{pw}}(\mathbf{x}_I) i^k e^{-ik \alpha_{\text{inc}}} J_k(\kappa \mathbf{r}_I).$$

Well-posedness

$$0 \leq \kappa_e < \infty \quad ; \quad \lambda \in \mathbb{R} \quad ; \quad 0 \leq \kappa_{\text{int}} < \infty, \quad 0 < \mu < \infty, \quad \mu \neq 1.$$

If κ_e^2 is not a Dirichlet eigenvalues (EV) of $-\Delta$ for \mathcal{O}_I for $1 \leq I \leq N_{\text{Obs}}$,
then \mathbf{A}_α is injective for $\alpha = \text{D, N, Imp, T}$.

Circular obstacles

$$\text{Dirichlet EV : } \lambda_{n,m} = \left(\frac{j_{n,m}}{r} \right)^2,$$

$j_{n,m}$ m -th positive root of $J_n(r) = 0$,

r = radius of obstacle.

$$\text{Injectivity : } \kappa_e^2 r^2 \neq j_{n,m}.$$

General shape obstacles

Isoperimetric inequality gives

$$\lambda_1(\mathcal{O}) \geq \frac{\pi}{\text{Area}(\mathcal{O})} j_{0,1}^2.$$

$$\text{Injectivity small obs. : } \kappa_e r_{\text{circumvent}}(\mathcal{O}) < 2.$$

The first 4 roots :

$$j_{0,1} \sim 2.40, \quad j_{1,1} \sim 3.83, \quad j_{2,1} \sim 5.13, \quad j_{1,2} \sim 5.52.$$

Plan

2 Comparison with Finite Element Method

Calculation time costs

$$u_{h,\text{scatt}}(x) = \frac{i\pi}{2} \sum_{J=1}^{N_{\text{Obs}}} \mathbf{r}_J \sum_{l=-\mathbf{m}}^{\mathbf{m}} V_{J,l} H_k^{(1)}(\kappa r_J(x)) e^{il\theta_J(x)} \quad (\star)$$

Unknowns $V_h = (V_{J,l})$, $1 \leq J \leq N_{\text{Obs}}$, $-\mathbf{m} \leq l \leq \mathbf{m}$.

Pre-processing time = Time to resolve the linear system for V_h .

Linear system is dense but small : $N_{\text{Obs}} \times (2\mathbf{m} + 1)$.

Post-processing time = Eval. time of LHS of (\star) at each point of visualization grid.

Evaluation of Hankel is costly.

- Cost increases with N_{Obs} and # points of visualization grid.
- Can reduce the cost by **parallelization** and interpolation (e.g. **Hermite interpolation**).

Experiment 1: Small obstacles on medium domain

Soft-scattering of PW with angle 90°

of wavelength $\kappa = 10$, $\lambda \sim 0.63$

by 200 obstacles

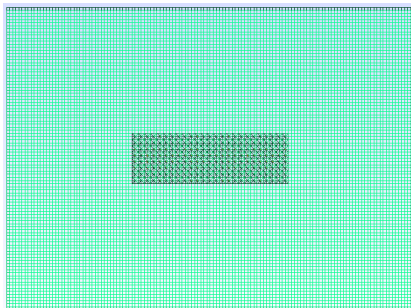
of radius = 0.03, with distanced by 0.3.

Domain size : $31\lambda \times 23\lambda$

$\kappa \times (\text{Obs Rad}) = 0.3$,

$\frac{\lambda}{\text{Obs Rad}} \sim 21$, $\frac{\lambda}{\text{Obs. Dist.}} \sim 2$,

$\frac{\text{Obs. Dist.}}{\text{Obs. Rad.}} \sim 10$.



Montjoie initial mesh has mesh size of 0.13.

Montjoie

(montjoie.gforge.inria.fr)

Bases: Curved finite element (FE) with Lagrange polynomials based on Gauss-Lobatto points.

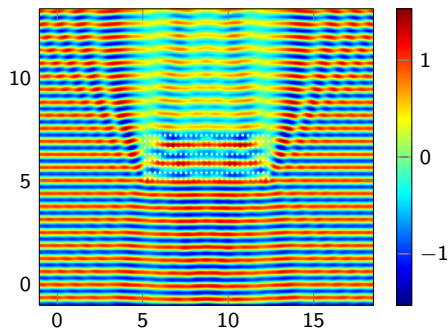
Q-n denotes the n^{th} order FE on quadrangular meshes.

Domain truncation: Perfectly Matched Layers.

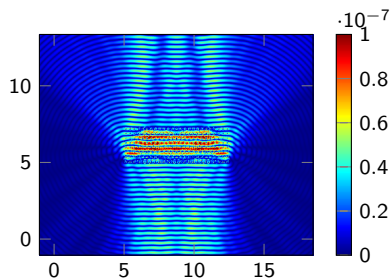
Experiment 1: Reference solutions

Soft-scattering of 200 obstacles on domain of size : $31\lambda \times 23\lambda$

$$\kappa \times (\text{Obs Rad}) = 0.3, \quad \frac{\lambda}{\text{Obs Rad}} \sim 21, \quad \frac{\lambda}{\text{Obs. Dist.}} \sim 2, \quad \frac{\text{Obs. Dist.}}{\text{Obs. Rad.}} \sim 10.$$

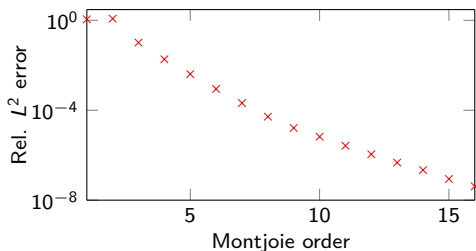


(a) Real part of FSSL 14 total wave

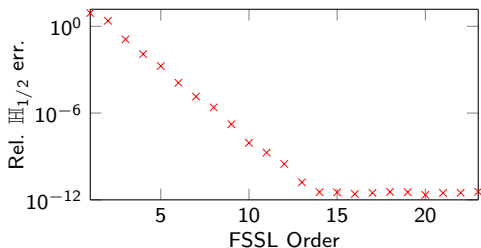


(b) Abs. difference compared with Montejoie Q17. Relative L^2 err. = 3.38×10^{-8} .

Experiment 1: Convergence curve



(c) Rel. consecutive err. : Montjoie



(d) Rel. consecutive err : FSSL densities

Candidates for comparison at precision 10^{-3}

Compare between		Rel. L^2 error
FSSL 14	FSSL 2	4.65×10^{-5}
MJ Q17	MJ Q6	6.52×10^{-4}
MJ Q6	FSSL2	6.84×10^{-4}

Hermite interp. precision is 10^{-6} .

Compare between		Rel. L^2 error
FSSL 2 Inter	FSSL 2	1.76×10^{-5}
FSSL 2 Inter	MJ Q6	6.85×10^{-4}

Solvers for both Montjoie and FSSL are Mumps.

Experiment 1: Comparison at precision 10^{-3}

Pre-processing by Mumps	FSSL Order 2	MJ Q6
Size of lin. sys.	1000	842677
Task	Time (s)	
Construction	0.055	1.97
Factorization	0.44	29.8
Resolution	0.003	0.35
Total time	0.498	32.12

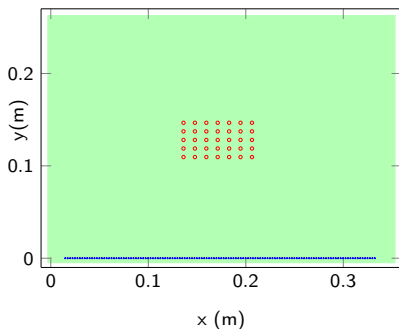
Evaluation on 400×400 grid

	Exact eval	Inter. eval	MJ Q6
Post-proc.	26.2	4.30	0.72
Pre-proc. + Post-proc.	26.70	4.80	33.82

At precision 10^{-3} , FSSL using Hermite interpolation takes 7 times less than MJ.

Experiment 2: sizable obstacles on a large domain

Acoustic vibration, produced by a block transducer , is diffracted by 35 thin aluminum wires • (of radius 0.5 mm) immersed in water.



Horizontal-view cut.

The phenomenon is approximated by the **hard scattering** of acoustic sound in fluid.

The incident wave (from the transducer) is simulated by a PW of angle 90° .

Input pulse's central freq. = 500 kHz.

The speed of sound in water $c = 1478 \text{ m s}^{-1}$.

The wavenumber $\kappa = 2125.57 \text{ m}^{-1}$.

The spatial wavelength $\lambda = 2.96 \times 10^{-3} \text{ m}$.

Domain size = $117\lambda \times 87\lambda$.

$$\kappa \times (\text{Obs Rad}) \sim 1.1, \quad \frac{\text{Obs Dist}}{\text{Obs Rad}} \sim (23, 19),$$

$$\frac{\lambda}{\text{Obs Rad}} \sim 5.91, \quad \frac{\lambda}{\text{Obs. Dist.}} \sim 0.3.$$

Exp 2: Computational time comparison at precision 10^{-4}

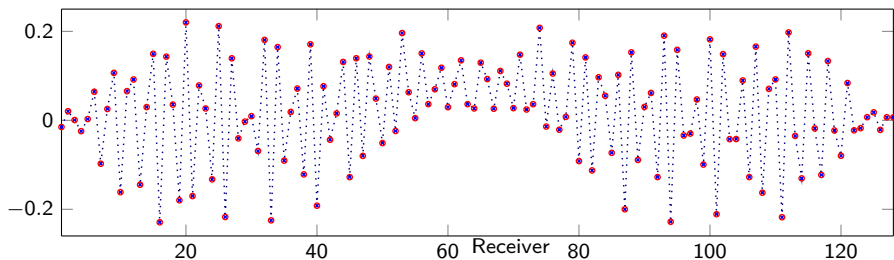
Regarding the value of the diffracted wave at 128 receptors,

Rel. L^2 error : FSSL 12 and FSSL 4 = 2.82×10^{-6} ,

Rel. L^2 error : MJ Q12 and MJ Q8 Ref 2 = 1.42×10^{-4} .

Rel. L^2 error : FSSL 4 and MJ Q8 Ref 2 = 1.48×10^{-4} .

Q8 Ref 2 = Q8
with one time
mesh refinement.



Real of part of diffracted wave at 128 receptors : FSSL 4 $\cdots \times \cdots$ and MJ Q8 Ref2 \circ .

Exp 2: Candidates for comparison at precision 10^{-4}

	Size of LS	Pre-proc. Time (s)	Post-proc. Time at 128 receivers (s)	Total time (s)
FSSL 4	315	0.024	6.58×10^{-3}	0.031
MJ Q8 Ref 2	993870	61.27	0.13	61.4

FSSL using Hermite interpolation is 2046 times faster than MJ.

Plan

- 3 Solver's robustness comparison
 - Closely spaced obstacles
 - Far away obstacles

Restart GMRES (generalized minimal residual method)

Consider $Ax = b$, A matrix of size $N \times N$.

Minimal poly $\Rightarrow A^{-1}b \in K_n(A, b) := \text{span}\{b, Ab, \dots, A^{n-1}b\}$.
Krylov space

For $d \leq m$, Arnoldi process constructs

$$AQ_d = \underbrace{Q_{d+1}}_{\text{orthonormal, } N \times d} \bar{H}_d; \bar{H}_n = \begin{pmatrix} H_d & \\ & 0_{1 \times (d-1)} h_{(d+1)d} \end{pmatrix}.$$

H_d Hessenberg of size $d \times d$

$$\|Ax - b\|_2 = \|AQ_d y - b\|_2 = \|\bar{H}_d y - \|b\|_2 e_1\|_2.$$

A sequence of approx. sol.

$$x_d = \underset{z \in K_d(A, b)}{\operatorname{argmin}} \|Az - b\|_2.$$

$$\Leftrightarrow y_d \text{ with } x_d = Q_d y_d$$

$$y_d = \underset{y \in \mathbb{R}^d}{\operatorname{argmin}} \|\bar{H}_d y - \|b\|_2 e_1\|_2.$$

Fixed Krylov size m . Initial guess (IG) x_0 . Initial residue $r_0 = b - Ax_0$.

No preconditioning : $A p_\star = r_0$.

For $j \leq m$, approximate sol. $p_j \in K_j(A, r_0)$ minimizes

$$p_j = \underset{p \in K_j(A, r_0)}{\operatorname{argmin}} \|Ap - r_0\|_2 \quad (*).$$

Stop if p_j satisfies the **residue error criteria**.

If not, and if $j = m$, restart the process with IG $r_0 = p_m$.

Final stop criteria : **NiterMax**.

Right preconditioning

$$(AP^{-1})(Pp_\star) = r_0.$$

Left preconditioning

$$(P^{-1}A)p_\star = P^{-1}r_0.$$

GMRES Preconditioners

L = strictly lower part of matrix A

$$M_u = U + D, N_u = -L$$

Splittings of A :

D = diagonal of matrix A

$$M_l = L + D, N_l = -U,$$

$$A = L + D + U = M_u - N_u$$

U = strictly upper part of A

$$R = -L - U.$$

$$= M_l - N_l = D - R.$$

The **backward Gauss-Seidel (BGS)** preconditioner is $\mathcal{P} = M_u$.

The **forward Gauss-Seidel (FGS)** preconditioner is $\mathcal{P} = M_l$.

The **Jacobi** preconditioner is $\mathcal{P} = D$.

The **Symmetric Gauss-Seidel (SGS)** preconditioner is

The **2nd-order Jacobi (2Jacobi)** preconditioner is

$$\mathcal{P} = D(R + D)^{-1}D.$$

$$\mathcal{P} = M_u D^{-1} M_l.$$

Interpretation: $u = \mathcal{P}^{-1}f$ solves

Formally, \mathcal{P}^{-1} is the 2nd approx. of the Neumann series of $A^{-1} = (D - R)^{-1}$.

$$M_u \tilde{u} = f, M_l u = N_l \tilde{u} + f.$$

The **2nd-order Forward Gauss-Seidel (2FGS)** preconditioner is

$$\mathcal{P} = M_l (N_l + M_l)^{-1} M_l.$$

The **Lower-Upper Symmetric Gauss-Seidel (LUSGS)** preconditioner is

$$\mathcal{P} = M_l D^{-1} M_u.$$

Formally, \mathcal{P}^{-1} is the 2nd approx. of the Neumann series of $A^{-1} = (M_l - N_l)^{-1}$.

Interpretation: $u = \mathcal{P}^{-1}f$ solves

$$M_l \tilde{u} = f, M_u u = N_u \tilde{u} + f.$$

Solvers in comparison

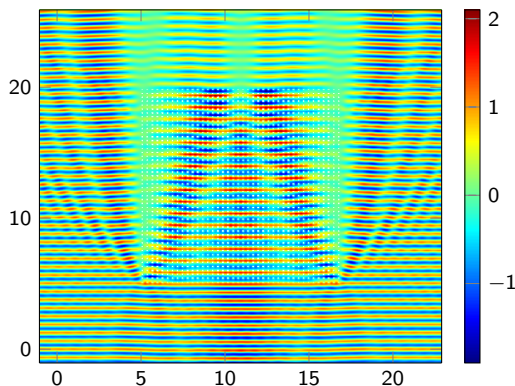
- Direct solvers : MUMPS, LAPACK, SCALAPACK.
- Code for GMRES solver is obtained from :

L. Giraud, et al. , *A set of GMRES routines for real and complex arithmetics on high performace computers*, Technical report, CERFACS, tR/PA/03/3 (1997).

The code allows user to define

- multiplication by the coefficient matrix.
- multiplication by a preconditioner with choices of positions.
- Parallel tests are run on cluster plafrim (www.plafrim.fr).

Closely-spaced obstacles comparison



FSSL order 2 with Mumps for 2000 obstacles.

Planewave (PW) with 90° .

Wavenumber $\kappa = 10$.

Radius of obstacle 0.03.

Distance btwn obs 0.3.

$$\kappa \times (\text{Obs Rad}) = 0.3;$$

$$\frac{\lambda}{\text{Obs. Rad}} \sim 21; \quad \frac{\lambda}{\text{Obs Dis}} \sim 2$$

$$\frac{\text{Obs Dist}}{\text{Obs Rad}} = 10.$$

GMRES stop criteria : Residue error tolerance, Niter Max, Size of Krylov.

Exp 4: Closely-spaced obstacles comparison (Dirichlet)

Name Method	Case 200 obstacles				Case 1616 obstacles			
	Cv	δ_{err} in $\mathbb{H}_{1/2}$	# Iter	Time (s)	Cv	δ_{err} in $\mathbb{H}_{1/2}$	# Iter	Time (s)
Mumps	n/a	0	n/a	0.05	n/a	0	n/a	130
Lapack	n/a	10^{-12}	n/a	0.01	n/a	10^{-10}	n/a	42.7
	GMRES stop criteria (10^{-6} , 2000,100)				GMRES stop criteria (10^{-6} , 2000,150)			
NoPreCond	Y	5×10^{-3}	820	0.09	N	n/a	n/a	n/a
L_Jacobi	Y	5×10^{-3}	656	0.08	N	n/a	n/a	n/a
L_FGS	Y	2×10^{-3}	239	0.05	N	n/a	n/a	n/a
L_BGS	Y	4×10^{-3}	197	0.04	N	n/a	n/a	n/a
L_2Jacobi	Y	5×10^{-3}	594	2.21	N	n/a	n/a	n/a
L_2FGS	Y	1×10^{-3}	169	0.1	N	n/a	n/a	n/a
L_SGS	Y	2×10^{-3}	76	0.03	Y	4×10^{-1}	757	274
L_LUSGS	Y	1×10^{-3}	77	0.03	Y	1×10^{-1}	897	325
R_Jacobi	Y	4×10^{-3}	660	1.05	N	n/a	n/a	n/a
R_FGS	Y	3×10^{-3}	199	0.05	N	n/a	n/a	n/a
R_BGS	Y	3×10^{-3}	198	0.04	N	n/a	n/a	n/a
R_2Jacobi	Y	4×10^{-3}	600	1.70	N	n/a	n/a	n/a
R_2FGS	Y	3×10^{-3}	155	0.09	N	n/a	n/a	n/a
R_SGS	Y	3×10^{-3}	75	0.03	Y	2×10^{-1}	886	321
R_LUSGS	Y	3×10^{-3}	74	0.03	Y	2×10^{-1}	897	325

Exp 5: Closely-spaced obstacles comparison (Dirichlet)

FSSL order =2 ; Size matrix = $10^4 \times 10^4$; GMRES stop criteria (10^{-6} , 5000, 400)

Solver	Post-proc (n16)	Rel $H_{1/2}$ diff	Rel L^2 diff	# iter	Preproc. time (s)	Postproc. time (s)	Total (s)
Mumps (n16)	Exact	3×10^{-10}	8×10^{-14}	n/a	242	96.0	338
Mumps (n16)	Inter	3×10^{-10}	9×10^{-6}	n/a	242	36.0	278
Lapack (n1)	Exact	0	0	n/a	80.4	96.0	176
Lapack (n1)	Inter	0	9×10^{-6}	n/a	80.4	37.5	118
R_LUSGS (n1)	Exact	1×10^{-1}	4×10^{-5}	1146	573	95.8	669
R_LUSGS (n1)	Inter	1×10^{-1}	4×10^{-5}	1146	573	36.2	609
R_SGS (n1)	Exact	1×10^{-1}	4×10^{-5}	1151	598	95.8	694
R_SGS (n1)	Inter	1×10^{-1}	4×10^{-5}	1151	598	36.2	635
Scala (n16)	Exact	3×10^{-10}	8×10^{-14}	n/a	34.6	95.6	130
Scala (n16)	Inter	3×10^{-10}	9×10^{-6}	n/a	34.6	36.1	70.9

PW of 90° ; $\kappa = 10.0$; $N_{\text{Obs}} = 2000$; Obs. Rad. = 0.03 ; Obs. Dist. = 0.30 ;

$$\kappa \times (\text{Obs Rad}) = 0.3, \quad \frac{\lambda}{\text{Obs. Rad}} \sim 21, \quad \frac{\lambda}{\text{Obs Dis}} \sim 2, \quad \frac{\text{Obs Dist}}{\text{Obs Rad}} = 10.$$

Exp 6: Far apart obstacles (Dirichlet)

FSSL order 2 ; Size matrix = 10000×10000 ; GMRES stop criteria (10^{-7} , 5000,500).

Solver	Post-proc (n16)	Rel $\mathbb{H}_{1/2}$ diff	Rel L^2 diff	# iter	Pre-proc. time (s)	Post-proc. time (s)	Total (s)
Mumps (n1)	Exact	0.0	0.0	n/a	251	96.0	347
Mumps (n1)	Inter	0.0	1×10^{-5}	n/a	251	37.5	289
Lapack (n1)	Exact	4×10^{-12}	2×10^{-15}	n/a	79.9	96.0	176
Lapack (n1)	Inter	4×10^{-12}	1×10^{-5}	n/a	79.9	37.5	118
R_LUSGS (n1)	Exact	3×10^{-4}	1×10^{-7}	57	37.5	96.0	134
R_LUSGS (n1)	Inter	3×10^{-4}	1×10^{-5}	57	37.5	37.5	75.3
R_SGS (n1)	Exact	4×10^{-4}	1×10^{-7}	56	37.0	96.0	133
R_SGS (n1)	Inter	4×10^{-4}	1×10^{-5}	56	37.0	37.5	74.6
Scala (n16)	Exact	1×10^{-11}	4×10^{-15}	n/a	34.9	96.0	131
Scala (n16)	Inter	1×10^{-11}	1×10^{-5}	n/a	34.9	37.5	72.5

PW of 90.0° ; $\kappa = 10.0$; # obs = 2000; Obs. Rad. = 0.01; Obs. Dist. = 2.00;

$$\kappa \times (\text{Obs Rad}) = 0.1, \quad \frac{\lambda}{\text{Obs. Rad.}} \sim 63, \quad \frac{\lambda}{\text{Obs Dist.}} \sim 0.3, \quad \frac{\text{Obs Dist.}}{\text{Obs Rad.}} = 200.$$

Plan

- 4 Application to inversion : initial results
 - No noise
 - 23dB Noise

Full waveform inversion

Minimize

$$J := \frac{1}{2} \|\mathcal{H}_{\text{rec}} u_{\text{scatt}} - d_{\text{obs}}\|^2 \quad ; \quad \hat{J}(p) = \frac{1}{2} \|\Phi(p) - d_{\text{obs}}\|^2 .$$

Optimization method : nonlinear conjugate gradient with Polak-Ribière coefficient.

Calculate **gradient** $\nabla_p \hat{J}$ by adjoint method (with FSSL formulation).

Trace operator at the receptors $\mathcal{H}_{\text{rec}} : u|_{\text{receptor}}, \partial_n u|_{\text{receptor}}, \text{etc.}$

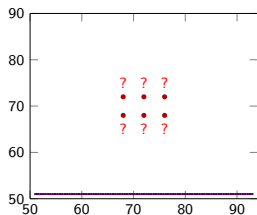
Observed data at receptors : d_{obs} .

Forward map $\Phi : \text{parameters} \mapsto \text{values at receptors.}$

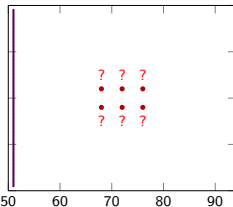
Acquisition Data

Inversion problem : Retrieve the position of 6 hard-scattering obstacles of radius 0.5 (distanced 3 and 4) placed at

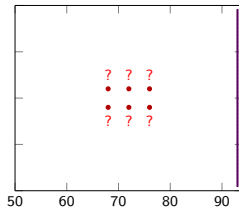
$(68, 68)$, $(68, 72)$, $(72, 68)$, $(72, 72)$, $(76, 68)$, $(76, 72)$.



(a) $\alpha_{\text{inc}} = 90^\circ$



(b) $\alpha_{\text{inc}} = 0^\circ$

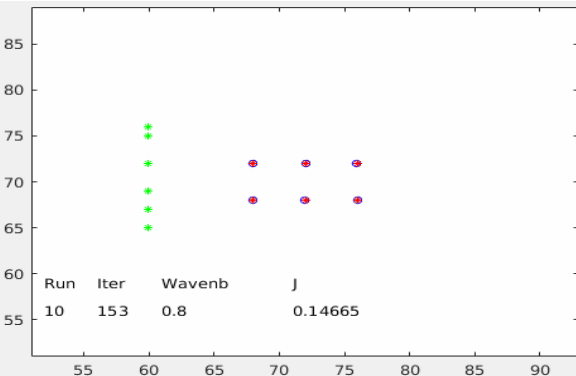


(c) $\alpha_{\text{inc}} = 180^\circ$

The position of 128 equally spaced receivers vary with the angle of incidence.

Data is produced by FSSL order 12 with solver Lapack.

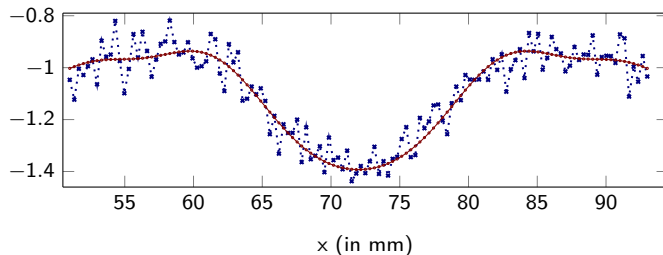
Reconstruction results using data with no noise.



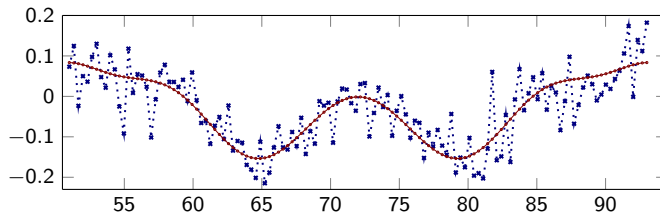
- ★ One angle of acquisitions: 90°
- ★ FSSL order 3 using Mumps .
- ★ Error Tolerance 10^{-5} .
- ★ Initial guess rel. error. : 115% (relative to size of domain).
Final position's rel. error : 1.3%
- ★ Initial J : 0.002 at $\kappa = 0.08$
Final J : 0.002 at $\kappa = 1.5$
- ★ Run time : 7.92 secs
- ★ Nb max linesearch (LS) 30.
Nb LS used in each run ≤ 11 .

Run	κ	# Niter Max	Step size	Run	κ	# Niter Max	Step size	Run	κ	# Niter Max	Step size
1	0.08	300	8	7	0.5	200	5	13	1.10	200	2
2	0.09	300	8	8	0.6	200	5	14	1.20	200	2
3	0.1	200	8	9	0.7	200	5	15	1.30	200	2
4	0.2	200	8	10	0.8	200	5	16	1.40	200	2
5	0.3	200	7	11	0.9	200	5	17	1.50	100	2
6	0.4	200	7	12	1.0	200	2				

Noise Data at 23dB



(a) Real part of total wave at 128 receivers at $\kappa = 0.8$ with PW 90°



(b) Imaginary part .

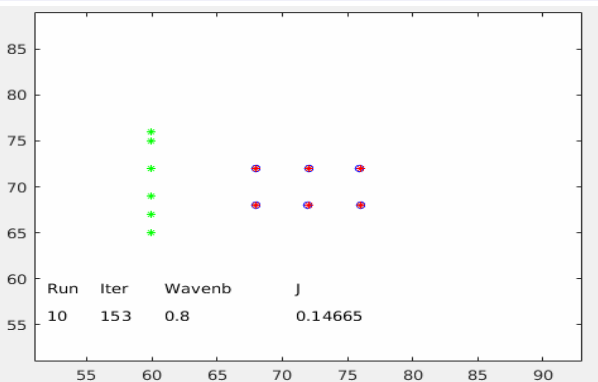
White
Gaussian noise
is added by
using wgn in
Matlab.

Rel. error in
norm

$$l^2 = 7\% ,$$

$$l^\infty = 18\%$$

Inversion result for data with 23dB noise

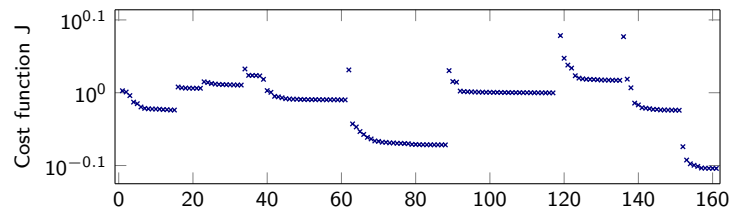


- ★ Three angles of acquisitions:
90°, 0°, 180°
- ★ FSSL order 3 using Mumps .
- ★ Error Tolerance 10^{-5} .
- ★ Initial guess rel. error. : 115%
(relative to size of domain).
- Final position's rel. error: 0.38%
- ★ Initial J 1.00 at $\kappa = 0.08$
- Final J: 0.79 at $\kappa = 0.7$
- ★ Run time: 2.79 secs

Run	κ	# Niter Max	Step size	Run	κ	# Niter Max	Step size
1	0.08	300	5	6	0.4	200	2
2	0.09	300	4	7	0.5	200	2
3	0.1	200	2	8	0.6	200	2
4	0.2	200	2	9	0.7	200	1
5	0.3	200	2				

Nb max linesearch (LS) 30.
Nb LS used in each run ≤ 10 .

Inversion result for data with 23dB noise (cnt)



★ Three angles of acquisitions:
90°, 0°, 180°

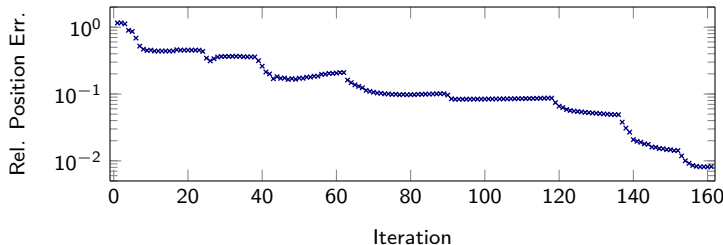
★ FSSL order 3
using Mumps;

★ Err. Tol. = 10^{-5} ;

★ Niter total = 161;

★ Use 9 κ s:
0.08, 0.09,
0.1, ..., 0.7

★ Run time: 2.79 s



Initial guess rel. err. = 115% (rel. to domain size); Final err. = 0.8%.

Conclusion

- ★ FSSL is robust in simulating the multi-scattering by **small circular obstacles** in **large homogeneous media**.
- ★ Its linear systems have simple expressions \Rightarrow Easy coding and implementation.
- ★ **Direct Solvers (Lapack and Scalapack)** are more efficient when the obstacles are close together.
- ★ Iterative solvers are more preferable when the obstacles are far apart. In particular, **GMRES with LUSGS and SGS are faster than Lapack and as fast as Scalapack**.
- ★ **LUSGS and SGS are the most robust among the preconditioners considered**.
- ★ In both settings, Scalapack is fastest.
- ★ Using shared memory architecture, Scalapack can handle the largest Nb of obstacles.

Further advantages of direct solvers, regarding application to inverse problem using Full waveform inversion

- multi-RHS, high precision
- the forward and adjoint problem use the same factorization.

Thank you for your attention